Cue to action processing in motor cortex populations

Naveen G. Rao and John P. Donoghue

J Neurophysiol 111:441-453, 2014. First published 30 October 2013; doi:10.1152/jn.00274.2013

Journal of Neurophysiology publishes original articles on the function of the nervous system. It is published 12 times a year (monthly) by the American Physiological Society, 9650 Rockville Pike, Bethesda MD 20814-3991. ISSN: 0022-3077, ESSN: 1522-1598. Visit our website at http://www.the-aps.org/.

J Neurophysiol 111: 441–453, 2014.
First published October 30, 2013; doi:10.1152/jn.00274.2013.

Cue to action processing in motor cortex populations

Naveen G. Rao and John P. Donoghue
Department of Neuroscience, Brown University, Providence, Rhode Island

Submitted 16 April 2013; accepted in final form 28 October 2013

Rao NG, Donoghue JP. Cue to action processing in motor cortex populations. *J Neurophysiol* 111: 441–453, 2014. First published October 30, 2013; doi:10.1152/jn.00274.2013.—The primary motor cortex (MI) commands motor output after kinematics are planned from goals, thought to occur in a larger premotor network. However, there is a growing body of evidence that MI is involved in processes beyond action generation, and neuronal subpopulations may perform computations related to cue-to-action processing. From multielectrode array recordings in awake behaving *Macaca mulatta* monkeys, our results suggest that early MI ensemble activity during goal-directed reaches is driven by target information when cues are closely linked in time to action. Single-neuron activity spanned cue presentation to movement, with the earliest responses temporally aligned to cue and the later responses better aligned to arm movements. Population decoding revealed that MI's coding of cue direction evolved temporally, likely going from cue to action generation. We confirmed that a portion of MI activity is related to visual target processing by showing changes in MI activity related to the extinguishing of a continuously pursued visual target. These findings support a view that MI is an integral part of a cue-to-action network for immediate responses to environmental stimuli.

motor cortex; action goals; visiomotor transformation; pursuit tracking

WE ROUTINELY USE VISION to initiate and guide goal-driven, volitional movements such as picking up a glass. To perform a goal-directed movement, the a perceptual representation of the action goal is transformed into a set of specific muscle activation patterns (Andersen et al. 1997; Buneo and Andersen 2006; Wolpert and Ghahramani 2000; Wolpert et al. 1995). Information about the action goal, such as its spatial location, must be mapped into a reference frame relevant to the effector limb to drive the limb to the target either immediately or after a delay (Andersen et al. 1997; Snyder et al. 1997). It is thought that multiple cortical networks perform this transformation, with the primary motor cortex (MI) positioned at the final stages of creating movement signals from an already highly processed sensory input and other internal signals (Ashe 1997; Kalaska and Crammond, 1992; Kalaska et al. 1997; Lamarre et al. 1983; Scott 2003). It is well established that MI is linked to the generation of voluntary arm movements (Ashe and Georgopoulos 1994; Crammond and Kalaska 1996; Dum and Strick 1991; Georgopoulos et al. 1982, 1992; He et al. 1993; Morrow and Miller 2003) and receives information about upcoming actions from a collection of areas that process sensory cues (Cisek and Kalaska 2005; Crammond and Kalaska 2000; Hatsopoulos et al. 2004; Schwartz et al. 2004). Evarts, Cheney, Fetz, and Humphrey classified MI activity into early phasic and tonic portions (Cheney and Fetz 1980; Evarts and Fromm 1981; Evarts and Tanji 1974, 1976; Humphrey et al. 1970; Tanji and Evarts 1976). They interpreted this early phasic activity as motor "set" related activity (Evarts and Tanji 1974; Tanji and Evarts 1976) or fast torque ramp up (Cheney and Fetz 1980), all related to preparing muscles and/or spinal cord for imminent movement. However, data from a number of approaches suggest that MI is engaged in perceptuomotor processing, including the activation of MI neurons by imagined action in people with paralysis, the influence of upcoming actions on ongoing discharge (Ashe et al. 1993), and activation of MI neurons when viewing learned actions (Dushanova and Donoghue 2006, 2010; Mukamel et al. 2010; Tkach et al. 2007, 2008). MI neurons contain processed task-relevant sensory information (Alexander and Crutcher 1990; Lamarre et al. 1983; Salinas and Romo 1998; Shen and Alexander 1997) and correlates of cognition (Georgopoulos et al. 1993; Sanes and Donoghue 2000) even when no movement has occurred (Hochberg et al. 2006; Moritz et al. 2008). Furthermore, Alexander and Crutcher (1990) and others (Hatsopoulos and Suminski 2011; Salinas and Romo 1998) have provided evidence for a role of MI in sensorimotor transformations. These findings suggest a richer role for MI in goal-directed behavior outside of movement generation.

The goal of this study was to address this conflict by providing evidence for a unified interpretation of the seemingly disparate roles of MI in movement generation and perceptuomotor processing. Multielectrode array (MEA) recording techniques make it possible to demonstrate the temporal evolution of cue to action processing in neural populations. The timing and response features of the simultaneously recorded population can be directly compared across cells, and collective network state changes can be evaluated by population decoding methods. In this study, we used MEA recordings during visually cued, manual step tracking, and pursuit tracking movements to examine the differences in information in early and late activity. Three findings demonstrate that the early activity reflects the intermediate processing of sensory-to-motor signals, whereas later activity is related to performed action. First, a subset of MI neurons showed tighter temporal coupling of firing rate changes to cue presentation than to movement onset. At the population level, we demonstrated that the early part of step tracking responses was cue related because it coded cue direction similarly regardless of whether an immediate movement occurred. Second, the population representation of the cue direction evolved temporally from cue presentation to movement onset, revealing different network states over time. This is not compatible with a fixed movement plan simply invoked by a cue. Third, we demonstrated that the visual presence or absence of the target during pursuit tracking affected MI firing rates, suggesting that this information may be used in MI to create or modify movement commands. This evidence places MI as a participant not only in generating

Address for reprint requests and other correspondence: N. Rao, 11087 Caminito Alegra, San Diego, CA 92131 (e-mail: naveen_rao@brown.edu).

action but also in the ongoing transformation of cue to action and further reinforces its role in perceptual processes in which sensory cues signal immediate action.

MATERIALS AND METHODS

Data were collected from MI in two adult *Macaca mulatta* nonhuman primates (NHPs: 1 male, AB; and 1 female, LA) using Blackrock MEAs (Fig. 1). For step tracking experiments (with C1 and C2 cues, Fig. 1), 6 sessions from each monkey were recorded for a total of 12 sessions. In half of these sessions (3 each), NHPs performed pursuit tracking with target blanking. Each recording session lasted ~1 h. Protocols for the veterinary care of the animals included in the study have been developed in conjunction with and approved by the Brown University Institutional Animal Care and Use Committee. All animals were maintained in a National Institutes of Health-approved animal care facility on the campus of Brown University. All surgical and experimental procedures were performed in this facility. As with other chronic MEA recording studies, we recorded three to six sessions per monkey as is accepted using MEA (Hatsopoulos et al. 2007; Mulliken et al. 2008; Tkach et al. 2007; Vargas-Irwin et al. 2010).

Experimental setup. NHPs were seated in a chair with their right arm secured in a custom-designed fixture attached to a Kinarm device (BKIN Systems, Ontario, CA). The Kinarm is a mechanical exoskeleton that constrains movement to a two-dimensional plane by only allowing elbow flexion and shoulder rotation about two fixed articulation points (Scott 1999). Elbow and shoulder joint angles were digitally (200 Hz) sent to a computer running Microsoft Windows XP. Custom software written in our laboratory drove the task stimulus and calculated a hand end-point position (tip of middle finger) from joint angles. This was used to drive a cursor on a vertical 40 × 32-cm (1280 × 1024 pixels) screen placed 45 cm from the monkey's eyes (1 cm = 1.27° of visual angle).

Task and animal training. NHPs were trained in a task that included both manual step tracking and pursuit tracking (Fig. 1). The step tracking component was used to temporally segregate the relationship between cues and movements, whereas the pursuit tracking component tested the ongoing influence of target on MI activity. Throughout the task, the hand position feedback cursor was a light blue dot (1 cm in diameter) and the target was either a purple or yellow dot 1.1 cm in diameter. When the hand cursor was within an acceptable diameter of the target (variable depending on phase of task), the target changed color from purple to yellow, signaling to the NHP that the correct target had been acquired.

Each trial always started with manual step tracking. The NHPs were trained to acquire the center target and hold for 1,000–2000 ms (center hold). The acceptable diameter for acquiring the target was 1.5 cm centered on the target. The trial would reset if the hand position cursor was moved outside the acceptable diameter or if the speed of movement exceeded 1.5 cm/s on screen during the hold. After this hold period, a new target, the C1 target (1.1 cm in diameter, purple in color) appeared at the periphery (4.3 cm on screen from the center target). The C1 target indicated the direction for an impending (but not immediate) movement. The C1 target was extinguished after 300 ms. After another 700–1,200 ms, the C2 peripheral target, identical to the C1 in form and color, appeared in the same position as the previous C1 target and the center target disappeared simultaneously. The combination of the appearance of the C2 target and the disappearance of the center target was the go cue. The NHP was then required to acquire C2 within 1,200 ms and hold the C2 for 1,000–1500 ms, or the trial would reset. After the required C2 hold period, the monkey received a juice reward. This combination of C1 with no movement and C2 with movement allowed us to observe and separate cue only-related activity (C1) from cue and movement-related activity (C2).

The next phase of the trial immediately following the C2 hold period was manual pursuit tracking. For this, the acceptable diameter for acquiring the target was increased to 2 cm (centered on target), but the viewed target was unchanged from step tracking (1.1 cm in diameter, yellow when captured and purple when not). After the C2 hold interval, the target moved smoothly in straight lines with a randomized Gaussian speed profile. The time of peak speed (6.25 cm/s) was randomized (from 0.8 to 1.2 s after start of target movement) to require the monkey to use visual guidance to follow the target. The target moved between the eight radial step tracking end

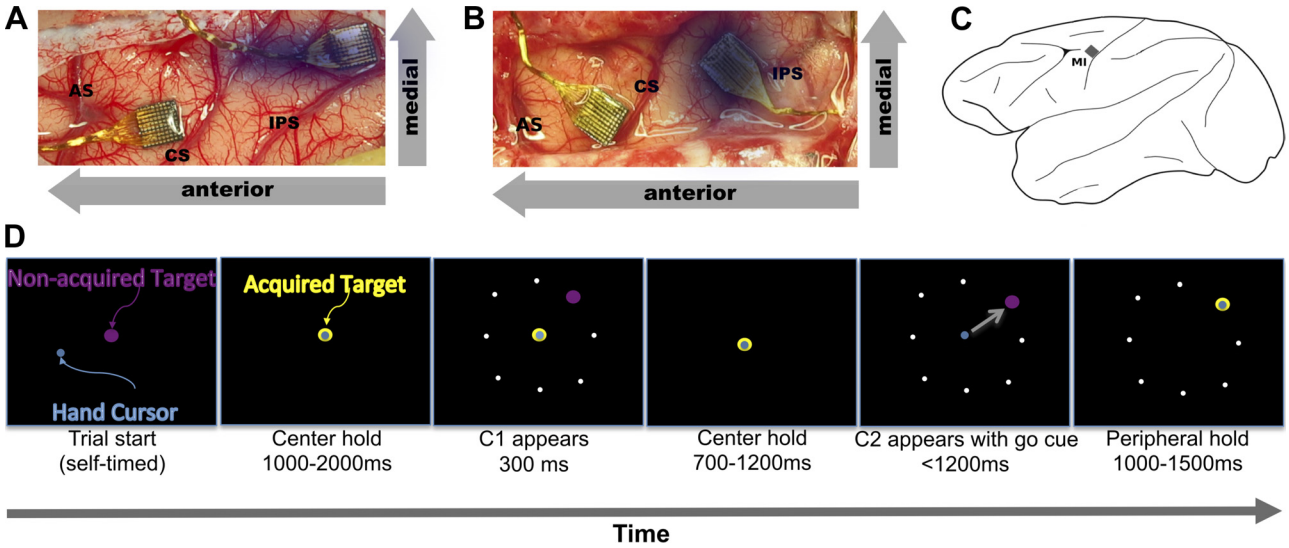

Fig. 1. Electrode implant sites and step tracking task description. *A* and *B*: implant sites for monkeys AB and LA, respectively. CS, central sulcus; AS, arcuate sulcus; IPS, intraparietal sulcus. The arrays for this study were placed in the arm area of primary motor cortex (MI) (along CS). The dimmed array was implanted in area 2/5 for another study. Each array is 4 mm on a side for scale. *C*: placement of the MI array. *D*: step tracking task. Throughout the task, the target is purple when unacquired but changes to yellow when the hand cursor is within the acceptable zone (acquired). Once the monkey has acquired the center hold target for 1,000–2,000 ms, C1 appears for 300 ms and is extinguished. The monkey must continue holding the center target during this time or else the trial will end immediately. After the center target is held for another 700–1,200 ms, C2 appears in the same position as C1, but the center target is extinguished simultaneously to indicate a movement (go cue). The movement must be completed in <1,200 ms, and the peripheral target must be held for 1,000–1,500 ms. White dots in the periphery are shown as positions of potential targets and are not seen by the monkey.

points along chords of an invisible circle (8.6-cm screen diameter, centered on the center target). Each trajectory (starting at one radial end point and moving to either a diametrically opposed end point or an end point adjacent to the diametrically opposed end point, chosen randomly) was 8–8.6 cm and took 3–4 s, depending on the speed and acceleration of the target. This process continued for 10–15 s for a total of 3–4 trajectories per trial. The monkey received randomly spaced rapid juice rewards (0.5–0.8 Hz) if the hand cursor was maintained within the acceptable diameter of the target. The monkey was motivated to continually follow the target by increasing reward frequency (up to 8 Hz) for longer periods of continuous target tracking. The trial did not end when the monkey released the target (out of the acceptable diameter); only the reward was stopped and the reward frequency was reset to the baseline.

During pursuit tracking, the target was extinguished for 300 ms on random trajectories, termed target blanking. Blanking always occurred at a target speed of 3 cm/s on the acceleration phase of the trajectory with a probability of 0.1–0.2 depending on the session. The NHPs were trained to continue moving the hand cursor as if the target were not blanked; they continued to receive increasing juice rewards, as in the paradigm described above, for tracking the invisible target within the defined acceptable diameter. This visual perturbation required that the NHP drive movement from an internal model of the target rather than relying on visual input.

Electrophysiology. Neural data were recorded using Blackrock Microsystems MEAs, chronically implanted into the MI upper limb area (just anterior to the central sulcus at the level of the genu of the arcuate sulcus) and area 2/5 (just dorsomedial to the intraparietal sulcus) of the two NHPs. The arrays in area 2/5 were not used in this study. Each array contained a 4 × 4-mm grid with 96 silicon-based electrodes with platinum tips 1 mm in length, spaced 400 μm apart (for details on array structure and surgical procedures, see Suner et al. 2005). The position of the arrays on the cortical surface in each monkey is shown in Fig. 1. Monkeys were head-fixed during recording. Data acquisition and storage were accomplished using a Cerebus multichannel data acquisition system (Blackrock Microsystems). Differences in spike waveform shape and amplitude were used to identify single-unit activity using custom software (Vargas-Irwin and Donoghue 2007). Within-animal recordings may have included overlapping populations (Hatsopoulos et al. 2007). The uniqueness of each population was impossible to establish definitively from day to day (Chestek et al. 2007; Dickey et al. 2009). Consequently, our analyses did not rely on independent samples. Properties pooled across sessions (as in Fig. 3) rely only on the populations being drawn from a similar distribution, not from independent samples. Monkey AB had 135 to 162 isolated units on the MI recording array, and monkey LA had 25 to 45 isolated units on the MI recording array across each session. Session data were collected 757–829 days postimplantation for AB and 37–59 days postimplantation for LA. Only neurons that showed a significant change of their spike rate [Kolmogorov-Smirnov (KS) test, $P < 0.005$] between a 300-ms bin before the go cue compared with any 300-ms bin (taken every 10 ms) from 0 to 1 s after presentation of the go cue were included in the data set. To determine whether a neuron's response contained direction information, a Kruskal-Wallis test ($P < 0.005$) was applied to the binned (100-ms bins) spike counts at a given time point.

State change index. To assess when a neuron's firing had changed state and the relative strength of this state change across trials, we developed a novel change point analysis method that produces an index of reliability of neural firing state change. Using a bootstrap method, we determined how reliably across trials the firing rate of neuron changed. This is done at multiple points in time (every 10 ms from 0 to 600 ms after go cue) after a repeated stimulus to produce an index of reliability of state change as a function of time. We call this index the state change index (SCI). For instance, to determine the SCI for a given neuron at t ms after the go cue, we bin the firing of that cell just before t and just after for each trial. The bin size for a given neuron was determined iteratively by finding the bin size that maximized the difference between the maximum and minimum SCI for the time interval (0 to 600 ms). Put another way, for a given neuron:

$$binSize = argmax\{\max\left[\mathrm{SCI}(binSize, t = 0..600\ \mathrm{ms})\right] - \min\left[\mathrm{SCI}(binSize, t = 0..600\ \mathrm{ms})\right]\}.$$

We then select a random subset of trials (called a subsample set) and determine if the bins before t are drawn from a different distribution from the bins after t using a KS test. This is repeated for a number of subsample sets (we used 1,000). The SCI (across-trial reliability) at time t is defined as the fraction of subsample sets in which there was a statistically significant difference between the bins before t and the bins after t. This is summarized as follows:

$$\forall_{i=1:m}:$$

$$b_t^i = \sum_{s=allSpikesTimes} (z_i + t - binSize) \le s < (z_i + t)$$

$$a_t^i = \sum_{s=allSpikesTimes} (z_i + t) \le s < (z_i + t + binSize)$$

where m = the number of trials in this subsample set; $Z = [z_1, z_2, \ldots, z_m]$, the trial-by-trial alignment times for this subsample set; $B_t = [b_t^1, b_t^2, \ldots, b_t^m]$, the binned spike counts before t for this subsample set; and $A_t = [a_t^1, a_t^2, \ldots, a_t^1]$, the binned spike counts after t for this subsample set.

The SCI at time t is defined as the fraction of the subsample sets that show B_t is drawn from a different distribution than A_t. The SCI is summarized as follows:

$$SCI_t = \sum_{allSubsampleSets} KStest\left(\left[b_t^1, b_t^2, \ldots, b_t^m\right], \left[a_t^1, a_t^2, \ldots, a_t^m\right] < \alpha\right)/(no.\ of\ SubsampleSets).$$

In our analyses, we randomly sampled 80% of the trials 1,000 times and used $\alpha = 0.005$ as our significance criteria. The null hypothesis is that spike counts before and after t are drawn from the same distribution, implying that no firing rate change occurred. With $\alpha = 0.005$ and 1,000 shuffles, it is expected that a process where no rate change occurred will have an SCI of no greater than 0.005 (5/1,000 shuffles). Our threshold for a significant firing rate change was an SCI of 0.1, well above that of a process with no state change. A threshold of SCI ≥ 0.1 proved to be a very stringent requirement for a firing rate change, because this criterion was never met in any recorded spike train during a period when no rate change should have occurred (e.g., while resting). In addition, we generated synthetic spike trains from a Poisson spiking process with fixed rates and found that none of them exceeded an SCI of 0.1.

This method has the distinct advantage of taking into consideration the trial-to-trial variability. Traditional change point analyses (Seal et al. 1983; West and Ogden 1997) operate on the average density of the process, i.e., the averaged PSTH in neural firing. If the response of the neuron is very regular across trials, these methods are adequate. However, neural firing responses can be highly variable from trial to trial, and these traditional methods do not deal well with that variability. We exploited this variability as a property of the cell, and this method provided a means to assess this variability.

Preferred raster alignment. Spike raster alignment is a standard method to visualize neuronal firing relationships. We determined each cell's preferred alignment using the SCI method delineated above. The preferred alignment is the event to which the transitions in firing rate of a neuron show the least variability from trial to trial. Therefore, the preferred alignment event is the event to which the neural activity is most temporally linked, although it does not address how persistent firing is related to other task features. This method determines the most reliable feature response across trials as the characteristic of comparison. Stated another way, the preferred alignment event has the least variability from trial to trial. The SCI was computed for each alignment of interest; in this study, we compared go cue alignments

(to detect visual target-related cells) to movement onset alignments (to detect kinematically linked cells). Movement onset was determined by first finding a speed threshold determined by the 99th percentile of movement speed evaluated at each of the 200-Hz samples 0–0.2 s after go cue (where it is certain no movement has occurred yet). The movement onset time was the time at which the movement speed exceeded the speed threshold for at least 100 ms. To make the lags comparable between the two alignments, we added the mean of the reaction times (RTs) to movement onset alignments:

$$\text{RTs} = (\text{movement onset times}) - (\text{go cue presentation times})$$

$$\text{Movement onset align times} = (\text{movement onset times}) + \text{mean RTs}$$

Shifting the timing of movement onset back by the mean of the RTs allowed us to assess a comparable neural lag of a neuron (detailed in *Lag assessment* below) in either alignment. We can therefore assess a lag in a cell's preferred alignment. The alignment with the highest maximum SCI (over some range of time after the alignment event, typically 0 to 600 ms every 10 ms, because this will cover the range of RTs) across trials was considered the preferred alignment of that neuron. A neuron was considered to have a significant preferred alignment if the maximum SCI of either alignment was greater than 0.1 and the difference of the maximum SCI for each alignment was at least 0.1. Note that all cells analyzed with the SCI method had been shown to be movement related by the criteria delineated above. An SCI of 1 means that a change of firing rate can be detected for every shuffle of trials, and an SCI of 0 means that no shuffle of trials had a detectable change of firing rate. The value of 0.1 was chosen because it represents a relatively high bar for rejection of spurious spike rate transitions (see *State change index* above).

Lag assessment. To find the point in time after some alignment event (such as presentation of go cue) that the neural firing rate changed most reliably, we again computed the SCI as a function of time. The lag was defined as the time of the maximum SCI in the preferred alignment of the neuron. The lag was used to determine the relative position of each cell in the transformation of cue to motor output.

Neural and kinematic classification. Classification of task condition (blanked or nonblanked trajectories) or task parameters (1 of 8 directions) was performed on both neural spiking data and kinematics data. Discrete classification was done with a soft-margin (cost = 0.4) support vector machine (SVM) classifier (Byvatov and Schneider 2003) using a radial basis function (RBF) kernel (gamma = 0.01). All classifications were done with a 10-fold cross-validation, so no data used for training the SVM are used during classification. For kinematic classifications, the speed, direction, acceleration, and jerk were used as dimensions for classification. Each kinematic parameter was sampled every 10 ms around the time of interest. For neural spiking classification, each neuron was binned at 100-ms overlapping bins every 10 ms. The spike counts for each bin for all neurons of a group were used as dimensions for classification. The cross-validated classification was done independently for each time point.

RESULTS

In this study, we evaluated the role of MI in the transformation of a visual cue into movement-related activity. Monkeys performed a task in which the cue first appeared without requiring action and then reappeared to become a movement cue (Fig. 1; see MATERIALS AND METHODS). Initially we used cue or movement alignment to determine whether responses were related more to cues or movement (see MATERIALS AND METHODS).

Neural activity aligns to visual presentation of cues. We established categories of task-related cells using the preferred alignment of single-cell firing to go cue or movement onset. Of the cells recorded from the 12 total sessions in this study, this analysis identified 3 types of neurons: go cue-aligned (GCA) cells, movement onset-aligned (MOA) cells, and intermediate-aligned (IA) cells. GCA and MOA neurons aligned best to their respective events, whereas IA cells did not align statistically better to either go cue or movement onset (maximum SCI $<$ 0.1 and/or difference of maximum SCI between go cue and movement onset is $<$0.1). Because IA cells fell somewhere between go cue and movement onset, they may have been engaged in the events spanning from cue to movement. IA cells all had movement-related activity but had no statistical difference between go cue or movement alignments. This pattern of alignments is consistent with the view that the MI population forms a continuum from cue activity through movement. For purposes of analysis we established the three alignment categories (GCA, MOA, IA), even though a continuum exists. Differences in alignment properties were particularly notable when RTs were variable; i.e., if there were no RT variability, there would be no difference in alignment, which may have made this effect difficult to detect in past studies. RT variability for monkey AB spanned from 100 to 745 ms (mean of 345 ms, variance of 13 ms), and that for monkey LA spanned from 195 to 663 ms (mean of 313 ms, variance of 6 ms). Figure 2 illustrates typical examples of the three alignments from each monkey, also showing end-point (hand) speed for all trials (gray lines) and the average (black line). For the *left* column, we added the RT mean from the movement onset time at *time 0* to more easily compare the time courses of this alignment with the *middle* column (GCA). Figure 2 illustrates how alignment reveals differences in cell firing relationships. Among all 6 sessions from monkey AB, we found that 45% of movement related neurons were GCA, 14% were MOA, and 41% were IA. Among the 6 sessions from monkey LA, the proportions of aligned cells were more similar across categories, with 34% GCA cells, 33% MOA cells, and 33% IA cells (see Table 1). Qualitatively, we noticed that most cells (~60%) have a component of their spiking activity that is GCA and a later component that is MOA; however, this was not specifically quantified. This mixing of GCA and MOA in a cell's response is not unlike phasic-tonic responses commonly seen in earlier studies in monkeys (Cheney and Fetz 1980; Evarts and Fromm 1981; Humphrey et al. 1970; Tanji and Evarts 1976). Furthermore, in this randomly selected population of MI neurons from cortical layers 3/5 accessible by our arrays (Schwartz et al. 2006), GCA cells were as common or more common than MOA cells or IA cells.

MI responses to C1 (without movement). The previous result linked the presentation of cue direction (C2) and movement onset in a defined temporal sequence, so the effect of the visual target alone on MI spiking could not be disambiguated. To understand if the early portion of these go cue-aligned responses was related to the action cue rather than movement generation, we analyzed the spiking activity around the presentation of the first cue, C1 (Fig. 1). The C1 cue instructed the same direction as the subsequent C2 cue, except C1 did not instruct immediate movement. Note that although C1 did not imply immediate action, it provided direction information about an impending movement. Since the go cue (appearance of C2 and simultaneous disappearance of center target) always followed C1, the monkey knew not to move during C1. Responses to C1 for MI neurons are shown in the right column

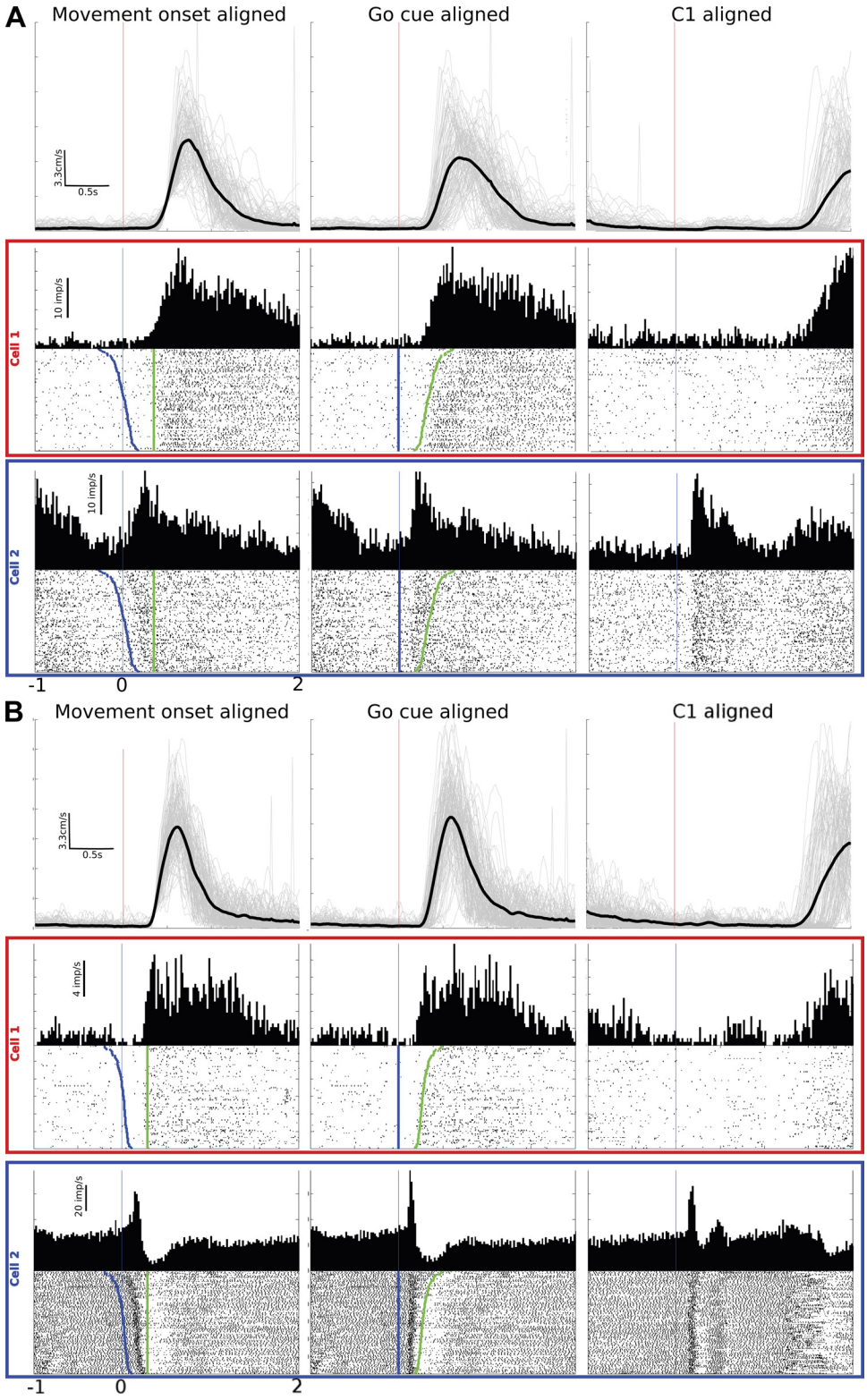

Fig. 2. MI responses to movement onset, go cue, and C1. Example cells are shown from monkey AB (*A*) and monkey LA (*B*). *Top* row of each diagram is the hand end-point speed with each trial's speed shown in light gray and the mean speed shown in heavy black. *Middle* and *bottom* rows are 2 example cells' responses. *Left* column is the movement onset-aligned response to go cue, *middle* column is the go cue-aligned response, and *right* column is the C1 response. Blue dots on the rasters are the presentation of go cue, and green dots are the onset of movement. Trials are sorted by reaction time.

of Fig. 2. Approximately 20% of all cells responded to C1 (monkey AB: 25 ± 3.66%, mean ± SE, range 34–11%, of cells pooled from 6 sessions; monkey LA: 19 ± 2.06%, range 27–14%, pooled from 6 sessions). About three-fourths of the cells showing a C1 response were also GCA (during C2), indicating that the C2 response contained C1 information. In monkey AB, of the 25% of cells that responded to C1, 75% were GCA, 13% were IA, and 12% were MOA. In monkey LA, of the 19% of cells that had a C1 response, 70% were GCA, 30% were IA, and 0% were MOA (Table 1).

For cells that were both GCA and had a C1 response, the magnitude of the C1 response was, on average, smaller than the go cue response. The majority of cells showed a significant increase in peak response to go cue. In monkey AB, 60% of

Table 1. *Summary of properties of cells from all sessions and both monkeys*

Session	No. of Cells with Movement Response	Movement Response, %					
		IA Cells	GCA Cells	MOA Cells	C1 Response	C1 Response and GCA	C1 Response and MOA
				Monkey AB			
100518	105	31	55	13	26	20	5
100520	125	34	52	14	31	22	5
100526	113	41	45	14	34	25	4
100701	111	34	50	15	30	25	3
100721	94	50	34	16	11	9	1
100729	100	50	37	13	17	9	1
				Monkey LA			
100805	25	20	32	48	12	12	0
100810	23	48	26	26	17	9	0
100817	22	32	32	36	14	9	0
100823	17	47	29	24	18	0	0
100825	22	32	41	27	27	27	0
100827	16	19	44	38	19	19	0

All percentages are taken from the total number of cells that met the criteria to have a step tracking response. IA cells, intermediate-aligned cells; GCA cells, go cue-aligned cells; MOA cells, movement onset-aligned cells. Two *right* columns show percentages of cells that have both a C1 response and are GCA or MOA.

cells showed an increase of >3 spikes/s in peak response to go cue (KS test, $P < 0.005$). In monkey LA, 71% of cells showed an increased peak response of >3 spikes/s difference. Furthermore, response latencies responses tended to be greater for C1 than for the go cue for cells that had a C1 response. The mean latency difference for monkey AB was 66 ms (± 57 ms SE), and that for monkey LA was 118 ms (± 67 ms SE). The distributions of latencies were statistically different (KS test, $P < 0.005$). These findings suggest that C2 may overlap C1 but that C2 is driven by additional input not present in C1.

Early engagement of GCA cells. Since GCA cells appeared to be initially driven by cue input (even when no motor output occurs as for the C1 response), we asked whether these same cells were the first to be engaged prior to movement. This cue-driven activity would be consistent with a role of MI in the transformation of a sensory-derived cue signal into a movement plan. For this analysis, we examined the relationship between the preferred alignment of a cell and its latency of spike rate change after go cue. Recall that comparisons within a session were made across cells that were recorded simultaneously, so the behavior, attention, and motivation were identical for each cell on a per-trial basis. The pooled comparisons for cells from all six sessions in each monkey are shown in Fig. 3. We found that GCA cells were engaged soonest after go cue (*time 0* in Fig. 3*A*), followed by IA and MOA cells. In both monkeys, the earliest GCA cells became active around 100 ms after cue, whereas the first group of MOA cells became active around 180 ms after cue (see Fig. 3*A*). Although the first IA cells were engaged around the same time as GCA cells, the majority of IA cells were engaged after the majority of GCA cells. The MOA cells (latency calculated when aligned to movement onset) were shifted forward by the mean RT to be compared with the GCA cells. In Fig. 3*B* we repeated the analysis but instead compared the neural-to-kinematic lags of the two populations. This movement onset-aligned analysis of lags yielded the same result as the go cue-aligned analysis; the GCA cells were first to be engaged, followed by IA and MOA cells.

The average response latencies from go cue and the average neural-to-kinematic lags for each population of cells (GCA, IA, or MOA cells) are summarized in Table 2. The distributions of latencies or lags for each population were statistically different ($P < 0.005$), and the mean of the GCA cells' latencies was earlier than the mean of the MOA cells' latencies by ~100 ms on average (100 ms in monkey AB, 101 ms in monkey LA). The latencies and alignments of these go cue-aligned responses suggest that cortically processed (presumably by visual or parietal areas) sensory information is used to initiate the computation of a movement plan in MI, consistent with implementing a portion of the sensorimotor transformation in this local network for response to real-time stimuli.

Similarity in direction coding for C1 and C2 responses. Individual MI cells were selectively responsive to cue direction for both C1 (no immediate movement) and C2 (immediate movement) with similar directional tuning for both cues (not shown). Given this finding, we next tested if there were similarities in the coding of direction across the population between the C1 response and the early part (~150 ms after cue presentation) of the C2 response (Fig. 4). We found that C1 evoked a similar pattern of activity in the population related to target direction as C2. That is, a multidimensional decoder trained on C1 responses predicted direction from C2 responses with high accuracy. This implies that the same ensemble direction code was operating both without (C1) and with (C2) immediate movement. In Fig. 4, the *x*-axis represents time points around C1 and the *y*-axis represents time points around C2. For each bin along the *x*-axis, we trained a discrete classifier for direction (8 directions) using binned neural data from each recorded neuron as predictor variables. This classifier was used to decode direction using binned neural data for the corresponding bins along the *y*-axis. For instance, at time 10 ms along the *x*-axis, we binned spikes for every recorded neuron 10 ms after C1 and used each of these as a multidimensional predictor for a direction classifier. Using this classifier, we then decoded direction from binned neural activity around C2 for every time point along the *y*-axis. The decoding performance (fraction of correctly decoded directions across trials) was indicated by the color of each point along the *y*-axis at $x = 10$ ms (with red = best decoding). This process was repeated for all points along the *x*-axis. In Fig. 4, if C1 and C2 responses coded direction in exactly the same manner, there

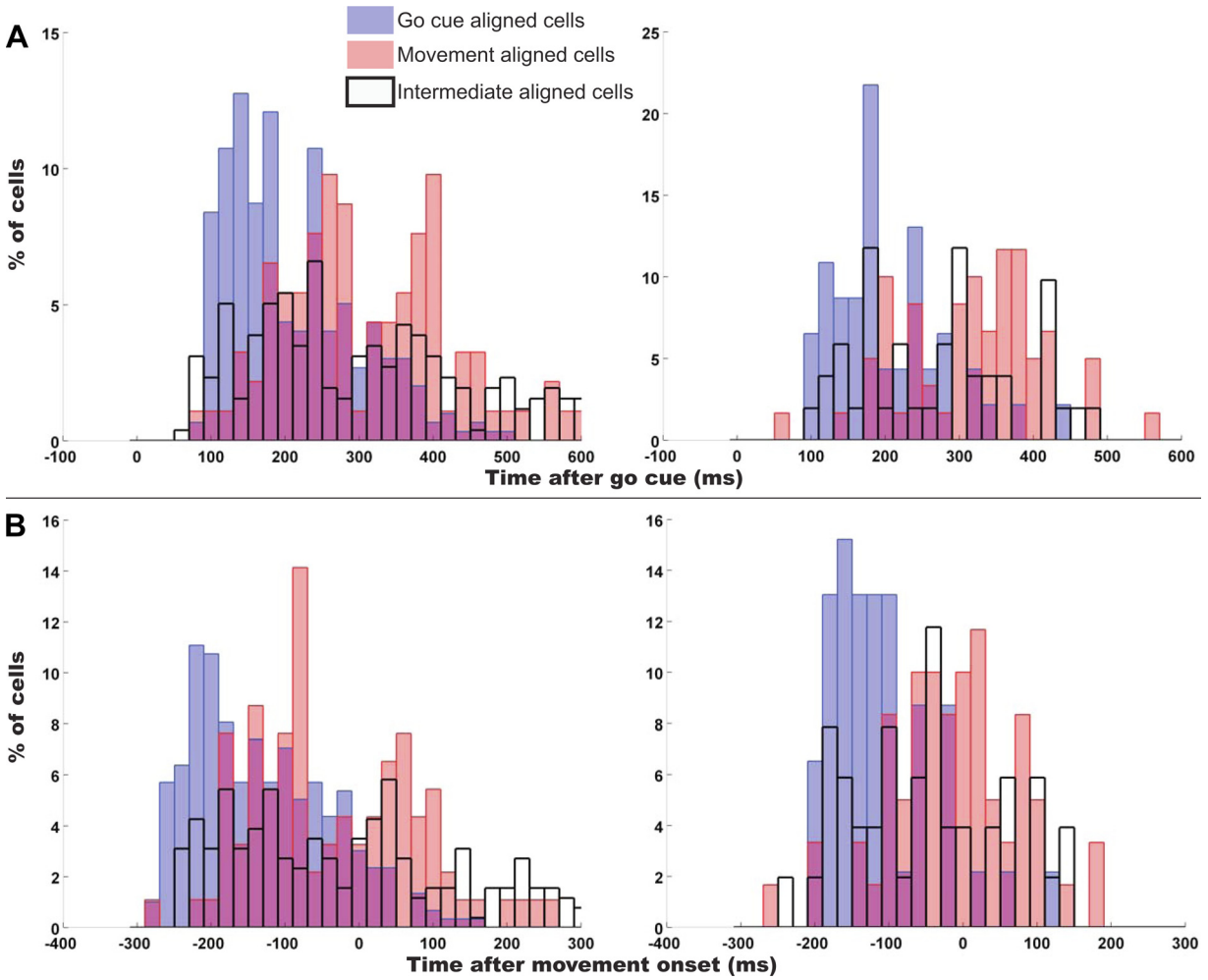

Fig. 3. Latencies and lags of cells with a preferred go cue alignment vs. preferred movement onset alignment. *Left* column is monkey AB, and *right* column is monkey LA. *A*: latencies from go cue presentation collapsed across sessions. *B*: lag from movement onset (negative implies before movement) collapsed across sessions. Blue bars represent the latencies and lags of cells with a preferred go cue alignment, and pink bars represent cells with preferred movement onset alignment (overlap is indicated by violet portions of bars). Black-outlined bars represent lags and latencies for intermediate aligned cells.

would be high decoding power where direction was represented similarly between C1 and C2. This analysis has the distinct advantage that it demonstrates not only that there exists similarity between C1 and C2 responses at the population level but also the temporal relationship between these similarities. As shown in Fig. 2, neural firing rate changes for individual cells occurred between 100 and 200 ms after C1 or C2.

Table 2. *Summary of properties for each population of cells from both monkeys*

	IA cells	GCA cells	MOA cells
Monkey AB			
Mean response latency after go cue, ms	288 ± 10.2	212 ± 5.1	312 ± 12.0
Mean neural-to-kinematic lag, ms	61 ± 10.5	134 ± 5.4	37 ± 12.1
Monkey LA			
Mean response latency after go cue, ms	267 ± 20.4	200 ± 11.9	301 ± 14.9
Mean neural-to-kinematic lag, ms	49 ± 20.3	114 ± 11.1	18 ± 14.2

Values are means ± SE.

Decoding direction from C2 responses with a model built from C1 responses (as in Fig. 4) increased beyond chance (0.52 for monkey AB and 0.4 for monkey LA) 100–200 ms after each cue. However, no movement occurred after C1, which was reflected in the observation that the decoding performance then dropped off quickly on both axes. Figure 4 shows data from monkey AB, and the trend for monkey LA (not shown) was similar.

Also overlaid on the plots in Fig. 4 as white and red lines is the direction decoding performance for C1 responses (white) and C2 responses (red) independently. Here, the decoding model was trained on the data that were decoded (either C1 or C2 responses), using leave-one-out cross-validation across trials with 100-ms bins. This shows the amount of direction information inherent to these responses within the respective condition (C1 or C2 response). The maximum decoding performance for C1 direction in the session shown was 0.61 for monkey AB and 0.31 for monkey LA; the maximum decoding performance for C2 direction was 0.77 and 0.36, respectively. We believe the lower decoding power in monkey LA was due to a smaller population of cells recorded. The observation that the maximum decoding performance across conditions (i.e.,

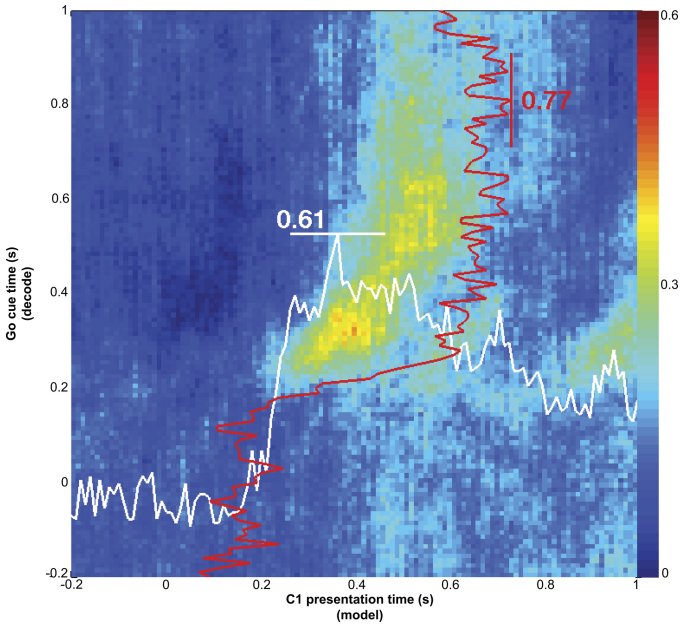

Fig. 4. Direction coding similarity between C1 and C2 responses. An 8-way discrete classifier model [support vector machine, SVM; radial basis function (RBF) kernel] for target direction was built from bins around the time indicated on the *x*-axis. Target direction was decoded from bins around the time indicated on the *y*-axis. The color of each point represents the fraction of correctly decoded trials for the time after C2 at the *y*-axis using a classifier trained on data from C1 at the time on the *x*-axis. Also shown is the cross-validated decoding performance of the C2 responses (red lines) and C1 responses (white lines) within their respective conditions. The origin for the red and white lines at *bottom left*. The existence of a region of high decoding power in this cross-condition (C1 to C2) decoding scenario suggests that C1 activity (along the *x*-axis) and the early part of the C2 activity (along the *y*-axis) code cue direction similarly across the population. Red and white lines show that each condition's responses (C1 or C2) also contain direction information. The maximum decoding power within the C1 condition (white line along *x*-axis) is 0.61, and the maximum decoding power within the C2 condition is 0.77 (red line along *y*-axis).

using C1 models to decode C2 responses) was similar to the within-condition performance (e.g., C1 to decode C1) further supports the hypothesis that arm direction is coded similarly between C1 and C2 across the population.

Time-evolving population coding of direction. The range of alignments (GCA to IA to MOA) and cue responses suggests that MI is involved in an evolving sensory-to-motor transformation from cue- into action-related activity. A sensorimotor transformation could be reflected in a change in the way the population codes action as arm movement is computed from its current position to the target. Others have observed that the preferred direction of individual cells changes through time (Churchland and Shenoy 2007; Hatsopoulos et al. 2007) and suggested that this finding reflects this serial computation process in MI. If the computation is evolving from sensory processing to movement planning, a decoding model created from population activity at one time in the trial would not apply later in the trial. In the prior section we demonstrated that the C1 responses were similar to the early part of the C2 responses. However, this similarity diminished within about 200 ms, because C2 was followed by an immediate movement whereas C1 was not. The population activity after C2 remained directionally selective (red lines, Fig. 4) while movement was underway. We next used population decoding to test whether early activity after C2 presentation represents direction similarly to later activity. Thus, if coding is changing, a model built early in the trial should fail to decode activity later in the trial. We tested this hypothesis using the same population cross-decoding technique as in Fig. 4. Discrete classifiers for direction (8 ways) were trained from the population neural spiking data (binned at 100 ms stepped every 10 ms) from 1 s before and 2 s after C2 shown on the *x*-axis. This classifier was then used to decode direction at each time point after C2 (using leave-one-out cross-validation) shown along the *y*-axis. The resulting analysis for both monkeys is shown in Fig. 5. The trend was for the region of high decoding performance to lie along the diagonal, indicating that the decoding model built at a particular time did not apply to other times. Rather, the initial population direction coding was different than it was later in

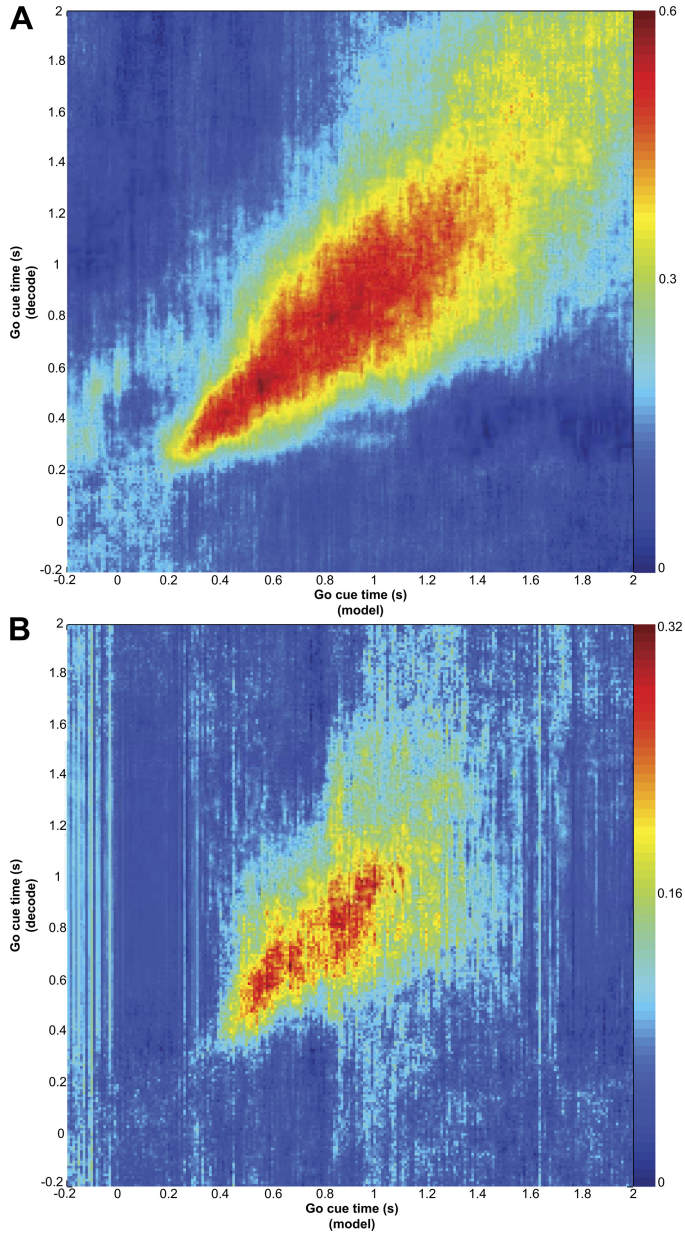

Fig. 5. Time-evolving direction coding after go cue/C2 for monkey AB (*A*) and monkey LA (*B*). Analysis is similar to that in Fig. 4 except here we compare go cue response to go cue response. Notice that most of the decoding power is shown to lie along the diagonal and not off-axis, indicating the population coding of direction is changing with time.

movement. Likewise, the population direction from later in the trial was different from earlier in the trial. Our finding demonstrates that the target direction is not a statically represented quantity in the MI ensemble and that the state of the MI network follows distinct trajectories for different movements (Churchland et al. 2006).

Blanking effects during pursuit tracking. The alignment and decoding results suggest that the early part of the neural activity preceding step tracking movements is related to the appearance of the cue that signals the spatial location (direction and extent) of the upcoming movement. It is difficult in step tracking movements to disentangle visual cue and movement because they unfold in close temporal proximity. To evaluate the role of the cue in supporting activity in MI, we used a pursuit tracking task in which monkeys were required to follow a target continuously. We then unexpectedly blanked the target to test whether activity was being driven by solely by motor output or was also being engaged by the presence of the target. This closed-loop task required that the motor plan be continually updated by vision of the target to continue accurate tracking. If the monkey successfully tracked the target for at least 1 s, and the target was on the acceleration phase of its trajectory, the target (but not the hand position feedback cursor) was randomly extinguished (blanked) for 300 ms. A trajectory segment in which the target was transiently extinguished was called a blanked trajectory. The invisible target continued to move as if it were visible and the monkey continued to receive reward if it kept the hand cursor within an acceptable zone of the invisible target. Note that the movements were predictable across this interval because they followed a slowly changing trajectory; successful tracking required a switch from reliance on visual feedback to an internal or learned model for successful ongoing tracking (Thoroughman and Shadmehr 1999; Wolpert et al. 1995). For comparison, we selected nonblanked trajectories that were direction and speed matched to the blanked trajectories as control trajectories. Since the target blanking occurred at the same target speed in all blanked trajectories, we could align the control trajectories to the same point in the target speed profile where the blanking occurred to compare the two.

The kinematics of both blanked trajectories and control trajectories are shown in Fig. 6*A*. Although it is nearly impossible for the blanked target to not affect the kinematics at the onset or offset of blanking (plus a reaction time; quantified below), it should be noted that the monkey continued to move through the blanked target in the same direction as the target. This demonstrated that the monkey retained and used some internal model of the predicted ongoing target features. This movement is far beyond what would be expected by simple inertia, since the Kinarm apparatus has very little mass and the arm's own internal resistance appears to halt movement immediately. What's more, inertia would be unlikely to move in the direction of the target due to anisotropies in the arm and Kinarm apparatus. Statistically there was no difference between the kinematics during the blanking period (KS test, $P < 0.01$) and a similar time in the control trajectories, although some behavioral changes were qualitatively evident in single trials after the blanked target reappeared. However, the diversity of neural responses at either the onset or offset of blanking is not explained by these behavioral changes. The response to blanking (Fig. 6*B*) in subsets of cells were remarkably mixed.

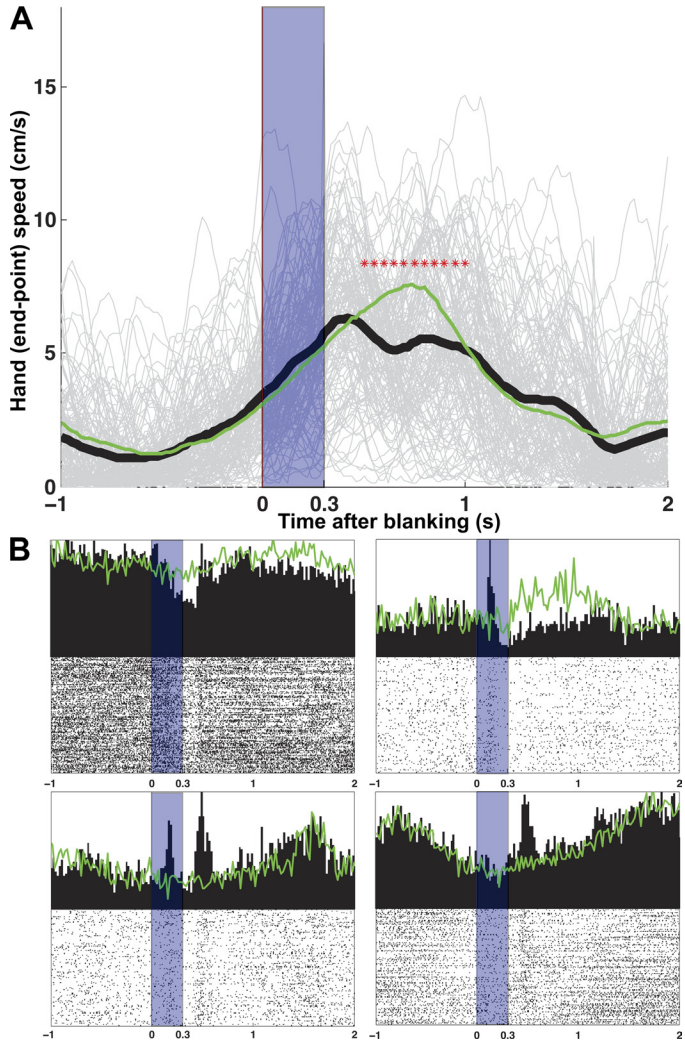

Fig. 6. Target blanking and neural responses. *A*: hand speed of pursuit tracking trajectories with target blanking at *time 0* (all directions). Individual trial speeds are shown in light gray and the mean in heavy black. Blanking period is indicated by the shaded area. Green line is the mean hand speed for nonblanked control trajectories. Asterisks indicate when blanked and control trajectories differ statistically. *B*: variety of neural responses. Four types of responses are shown: tonic (*top left*), phasic blanking onset (*top right*), phasic blanking onset/offset (*bottom left*), and phasic blanking offset (*bottom right*). Again, the shaded area indicates the blanking period and the green line shows the same neuron's mean response to the control trajectories.

They were either tonic (suppression or activation for the duration of the blanking) or phasic (transient response at the onset or offset of blanking) and maintained a strict temporal relationship with the onset/offset of visual blanking. Recall that all of these single-cell responses can be directly compared because cells were recorded simultaneously. The phasic responses were one of three types: at the onset of blanking only, at the offset of blanking only, or at both times. In monkey AB, 31% percent of movement-related cells showed one of these responses (tonic or phasic) to blanking, and 23% in monkey LA. The percentage of cells that both had a response to blanking and were GCA was 25% for AB and 10% for LA. The percentage of MOA cells that had a blanking response were 6% for AB and 14% for LA. Importantly, the activity of about two-thirds of cells (AB 69%, LA 77%) of the simultaneously recorded neurons remained unchanged during the blanking

period (compared with control trajectories), showing that many cells continue through blanking as if they were fully driven by an internal movement model unaffected by target feedback. The observation that responses were diverse diminishes the possibility that cells with altered firing were simply explained as a global change in motor behavior. This result suggests that a subset of MI cells contain information about the target, and their change in response between blanked and control trajectories could be reflective of a change from reliance on both an internal model and vision while the target is present to reliance on only an internal model when the target is extinguished.

Next, we found that GCA cells contained more information about blanking than did MOA cells. We tested this idea by evaluating whether a population model of GCA cells could better predict visual blanking than could a population model based on MOA cells. Recall that the step tracking portion of the trial preceded the pursuit tracking portion, so we were able to classify cells into their respective categories (GCA, IA, MOA) for each session, build a population classifier for each category, and directly compare their predictive power for visual blanking. We applied a cross-validated, multidimensional population classification method (see MATERIALS AND METHODS). The spiking data from all neurons during blanked and control trajectories were binned at 100 ms every 10 ms from 0.5 s before blanking (or equivalent alignment point for control trajectories) to 2 s after (Fig. 7). At each time point, the binned spike counts from each neuron in the population were used to classify whether or not they were observed during a blanked trajectory or control trajectory. All classifications were 10-fold cross-validated and controlled for the number of cells from each subpopulation (random subsampled, repeated and averaged). A 95% confidence interval was established by shuffling labels (shown in gray). The results for GCA cells and MOA cells are shown for one session for monkey AB in Fig. 7. Other sessions from this monkey and monkey LA exhibit a similar pattern. The maximum visual cue classification accuracy of GCA cells was 92% whereas that of MOA cells was 74% in both monkeys (subsampled neurons from each category, cross-validated decoding, and averaged), suggesting GCA cells contain more information about blanking than MOA cells. IA cells had a similar performance to MOA cells.

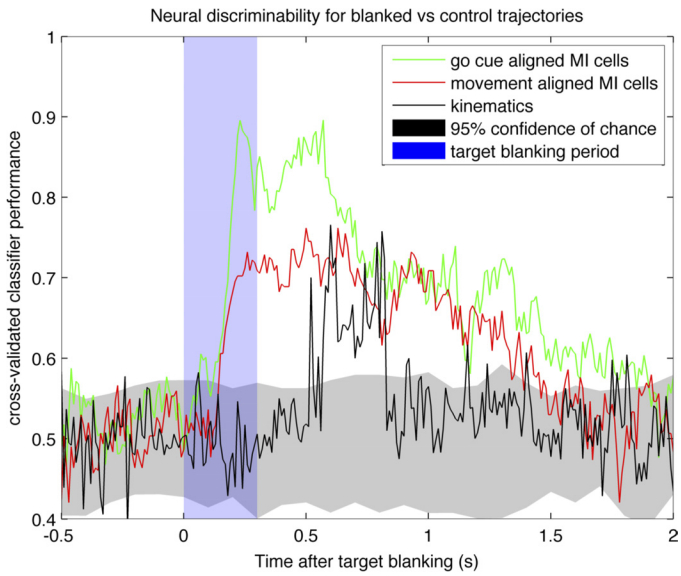

Fig. 7. Binary classification of blanked vs. control trajectories for neural spiking and kinematics. *Time 0* on the *x*-axis is the time of the target blanking for the blanked trajectories and the speed-matched point for the control trajectories. Black line indicates classification accuracy for kinematic parameters only; we used position, direction, acceleration, and jerk. Green line is the classification accuracy using spiking responses from cells with a preferred go cue alignment. Red line is the classification accuracy using spiking responses from cells with a preferred movement onset alignment. The classification accuracy of unaligned cells (not shown) is similar to that of movement-aligned cells.

To reject the hypothesis that differences in neural firing between blanked and control trajectories were simply due to differences in kinematic output, we used kinematic variables to decode whether a trajectory was blanked or not (heavy black line in Fig. 7). We computed the X and Y components of position, velocity, acceleration, and jerk for the hand for a total of 8 dimensions. Although we did not directly control the number of dimensions between kinematic (8 dimensions) and neural (>20 dimensions) classifications, we feel this is still a justified comparison since we are attempting to compare the amount of information about blanking in the two sources. In addition, measures of kinematics are far less noisy than binned neural data, so it is unlikely that there is any additional kinematic information to be gained by using multiple measurements (i.e., data from an accelerometer). If anything, the kinematic classification should produce a better representation of the true information content due to lower dimensionality with less noisy inputs. The kinematic values were taken every 10 ms, 0.5 s before blanking (or equivalent point for control trajectories) and 2 s after blanking (similar to the neural data classifications), and were used to classify whether or not the values were observed from a blanked or control trajectory (using 10-fold cross-validation). The results show that both subpopulations of cells (GCA and MOA) have greater classification power than the kinematics in classifying whether a trajectory was blanked, suggesting that the change in neural firing is not fully explained by differences in kinematics alone and that presence of target influences the responses of some MI cells.

DISCUSSION

Our results suggest that motor cortex is involved in ongoing sensorimotor transformations from cues that provide information about action goals, especially when responses to cues are closely linked in time. Our data show that the initial spiking responses in MI may be driven by the visual target presentation in preparation for possible movement. This spiking response subsequently evolves temporally and becomes increasingly related to the production of the upcoming movement. Four sets of evidence support this cue-to-action evolution in MI. First, at the individual cell level, the earliest activated cells are temporally best aligned to cue presentation (GCA) and latest activated cells are best aligned to movement onset (MOA), with a prominent intermediate class (IA) spanning the two events (Fig. 3). Second, population decoding showed an evolving direction code (Fig. 5), which transitions through different network states across time. Third, we found that MI neurons respond to a learned action target, even when that target did not cue an immediate movement. Fourth, using pursuit tracking, we revealed a subset of cells with activity that was affected by the presence or absence of a target. These were intermingled

with other neurons that were not affected by target presence. These analyses suggest that small ensembles of MI neurons participate in an unfolding computation that transforms cue information into a movement signal for immediate responses to visual stimuli. This broadens the notion of motor cortex from being a conduit to spinal motor circuits for premotor planning areas to one engaged in perceptual motor processes closely linked in time.

MI as a perceptual motor structure (viewed action). Our data suggest that the appearance of a cue for an impending movement produces a response that represents features of the cue not yet in a final movement framework. We defined cue cells on the basis of temporal organization, differences in response, and sensitivity to the presence of the cue. Cue cells were better aligned to cue appearance than to movement onset, indicating that this signal drove the activity. Variability in the reaction time helped reveal this dissociation. This cue-movement dissociation would be less evident in animals with less variance in reaction time. In addition, cue responses persisted in about half of the GCA cells when the cue was presented alone (C1; Table 1). The similarity of C1 and C2 direction coding at the population level suggests that both evoke a comparable MI state (Fig. 4). Recall that C1 and C2 cues are identical except that C1 only provides direction information about a future but upcoming movement (and does not cue immediate movement), whereas C2 both provides direction information and cues immediate movement. This would suggest that the C1 response and the beginning of the C2 response is a correlate of a motor plan that either did (C2) or did not (C1) result in motor output. Although not tested in this study, the C1 response in MI likely only occurs when the cue is meaningful in the context movement and is not a purely passive visual response. Alexander and Crutcher (1990) also showed that the majority of MI cells carry goal information that later shifts to movement information closer to movement onset. However, they did not demonstrate the population dynamics of direction representation evolving from action-cue presentation to motor output. Consistent with initial goal encoding, Salinas and Romo (1998) showed that sensory-driven responses were eliminated in MI (but not S1) when the stimulus had no meaning in the context of movement. Together, this evidence suggests that the C1 response and the early part of the C2 response include higher level perceptual responses reflecting action goals rather than either visual responses or motor output. Our study provides further evidence that temporally evolving MI activity during cued movements is related to the transformation of action-goals into motor plans.

The visual cue appeared to have a persistent influence on a subset of cells intermingled with sets of neurons apparently engaged in other aspects of a perceptuomotor transform. Thus, during pursuit tracking, about one-third of cells changed their activity when the target was transiently removed (Fig. 6). These responses were either phasic or tonic and maintained a strict temporal relationship to the onset or offset of blanking, suggesting a complex processing of the percept. With the use of population classification, GCA cells were more informative about blanking compared with MOA cells (Fig. 7), suggesting that sensorimotor transformations remain partially segregated within small ensembles of MI neurons, although this apparent segregation may have resulted from our classification scheme, which separated responders into three classes. Data from blanking classification performance (Fig. 7) showed that each subset of neurons (GCA, IA, or MOA cells) contained more information about the target than the actual behavioral output. This indicates there is an effect from viewing the target present in the neural activity that is not simply explained by the difference in kinematics between blanked and control trajectories. Given that we sampled a very small fraction of the total neurons present in MI, it implies there must be a robust effect of visual target on MI neural activity and that MI activity is related to factors beyond motor output.

Our recordings targeted the arm area of MI. As shown in Fig. 1, our MI array was placed in the rostral half of MI on the surface of the precentral gyrus. However, it did not sample the deeper, more caudal MI that is inaccessible using our method. Our sample might have encroached on premotor cortex (PM). However, our data suggest that this is not the case. Our cells were engaged around the time of movement, which is characteristic of MI. Cue-related cells are found in PM cortex, but C1 did not produce significant activity that carried across the delay to C2, which would have been a hallmark of PM cortex (Churchland et al. 2006; Cisek and Kalaska 2005). We also did not find that cue responses were more prevalent in the anterior parts of the array (which might be PM) but were intermingled everywhere. We found no functional difference in the cells recorded from the rostral and caudal parts of the recording array (not shown). It has been suggested (Crammond and Kalaska 2000; Rathelot and Strick 2009) that more rostral MI areas are involved in more abstract processing, whereas the caudal areas are related to specific muscle synergy patterns. Our data suggest that coding for perceptual and motor features are intermingled and contained within this rostral MI network.

Goal-related activity has previously been demonstrated in both PM and MI cortex. Cisek and Kalaska (2005) showed correlates of a decision process leading to one of two possible motor outputs in the dorsal premotor cortex (PMd). Information from two possible goals was simultaneously represented in PMd until the actual goal was clarified. This manifested as delay activity evoked by the presentation of the potential goals. Churchland et al. (2006) showed evidence of preparatory activity in both PMd and MI. They interpret this early goal-related activity to be the beginning stages of a motor plan evolving from an abstract goal, across time, to a concrete motor plan. Consistent with these previous studies, we interpret our results to be evidence of formation of this early motor plan for immediate responses to action goals in MI. Unlike prior studies, however, our task does not require the monkey to hold information across time, allowing us to directly compare activity after C1 (no movement) and C2 (with movement). Since MI tends to have less delay activity than PM (Crammond and Kalaska 2000) but has access to visual target information (presumably processed by other cortical areas) (Garcia-Rill and Dubrovsky 1974; Merchant et al. 2001; Wannier et al. 1989), MI may be capable of mapping this processed visual target information to a motor plan for immediate responses to stimuli, whereas premotor areas are specialized to couple these features across longer time frames. This may explain why target direction information quickly collapses when the monkey knows that no action is to be immediately produced in the C1 trials (Figs. 2 and 4). When actions require information to be integrated over longer time periods, however, other cortical areas are likely engaged with MI at the final stage mediating

short-term planning. These results support the idea that the frontal lobe is organized along a time axis in which areas near the central sulcus are more involved in immediate responses, whereas more frontal areas deal with spanning time gaps between a cue and future action.

Taken together, our results and previous studies suggest that there is an early movement goal influence in MI that is transformed to motor output within local MI networks. How does this transformation occur? There is a growing body of evidence that viewed action itself affects MI (Dushanova and Donoghue 2006, 2010; Mukamel et al. 2010; Tkach et al. 2007, 2008), during both passive observation (but still in the context of movement) and movement performance. In our task, it is important to note that there is an unambiguous mapping between the cue direction and the required movement, allowing MI to simply map cue direction to motor plan. As suggested by Paz and Vaadia (2004), the monkeys in our study likely optimized their cortex to use only networks required to complete the task. Since MI has access to processed sensory information (Garcia-Rill and Dubrovsky 1974; Hatsopoulos and Suminski 2011; Lamarre et al. 1983; Merchant et al. 2001; Wannier et al. 1989), we posit that this immediate mapping to a motor plan is computed in MI by perturbing the dynamical network state as suggested by Yu et al. (2006). The visual target (or abstract goal) would be the "kick" to the dynamical system that generates a unique state-space trajectory to complete the mapping from goal to motor plan. Our demonstration of an evolving network state (Fig. 5) supports this hypothesis. More complex tasks, with temporal delays, spatial mismatches, or higher cognitive demands, certainly engage other cortical areas, thereby allowing MI to associate processed sensory information with motor plans as suggested by Salinas and Romo (1998). There is evidence from past studies to support this interpretation of computation. Hatsopoulos et al. (2007) showed that individual MI cells code temporal sequences ("movement fragments") that may form a basis set for movement representation, but we interpret these temporal fragments to be a reflection of the cue-to-movement processing rather than simply action itself. Our findings imply that MI, like other cortical areas, is involved in computing action from perceptual signals rather than a simple cortical relay to the muscles.

GRANTS

Support is gratefully acknowledged from Department of Veterans Affairs, Rehabilitation Research & Development Service; National Institute of Neurological Disorders and Stroke (NINDS) Javits Award NS25074; NINDS Grant 1 F31 NS070485-01A1 (N. G. Rao); Defense Advanced Research Projects Agency; Katie Samson Foundation; and Craig H. Neilsen Foundation.

DISCLAIMER

The contents do not represent the views of the Department of Veterans Affairs or the U.S. Government.

DISCLOSURES

No conflicts of interest, financial or otherwise, are declared by the authors.

AUTHOR CONTRIBUTIONS

N.G.R. and J.P.D. conception and design of research; N.G.R. performed experiments; N.G.R. analyzed data; N.G.R. and J.P.D. interpreted results of experiments; N.G.R. prepared figures; N.G.R. drafted manuscript; N.G.R. and J.P.D. edited and revised manuscript; N.G.R. and J.P.D. approved final version of manuscript.

REFERENCES

Alexander GE, Crutcher MD. Neural representations of the target (goal) of visually guided arm movements in three motor areas of the monkey. *J Neurophysiol* 64: 164–178, 1990.

Andersen RA, Snyder LH, Bradley DC, Xing J. Multimodal representation of space in the posterior parietal cortex and its use in planning movements. *Annu Rev Neurosci* 20: 303–330, 1997.

Ashe J. Force and the motor cortex. *Behav Brain Res* 87: 255–269, 1997.

Ashe J, Georgopoulos AP. Movement parameters and neural activity in motor cortex and area 5. *Cereb Cortex* 4: 590–600, 1994.

Ashe J, Taira M, Smyrnis N, Pellizzer G, Georgakopoulos T, Lurito JT, Georgopoulos AP. Motor cortical activity preceding a memorized movement trajectory with an orthogonal bend. *Exp Brain Res* 95: 118–130, 1993.

Buneo CA, Andersen RA. The posterior parietal cortex: Sensorimotor interface for the planning and online control of visually guided movements. *Neuropsychologia* 44: 2594–2606, 2006.

Byvatov E, Schneider G. Support vector machine applications in bioinformatics. *Appl Bioinformatics* 2: 67–77, 2003.

Cheney PD, Fetz EE. Functional classes of primate corticomotoneuronal cells and their relation to active force. *J Neurophysiol* 44: 773–791, 1980.

Chestek CA, Batista AP, Santhanam G, Yu BM, Afshar A, Cunningham JP, Gilja V, Ryu SI, Churchland MM, Shenoy KV. Single-neuron stability during repeated reaching in macaque premotor cortex. *J Neurosci* 27: 10742–10750, 2007.

Churchland MM, Shenoy KV. Temporal complexity and heterogeneity of single-neuron activity in premotor and motor cortex. *J Neurophysiol* 97: 4235–4257, 2007.

Churchland MM, Santhanam G, Shenoy KV. Preparatory activity in premotor and motor cortex reflects the speed of the upcoming reach. *J Neurophysiol* 96: 3130–3146, 2006.

Cisek P, Kalaska JF. Neural correlates of reaching decisions in dorsal premotor cortex: specification of multiple direction choices and final selection of action. *Neuron* 45: 801–814, 2005

Crammond DJ, Kalaska JF. Differential relation of discharge in primary motor cortex and premotor cortex to movements versus actively maintained postures during a reaching task. *Exp Brain Res* 108: 45–61, 1996.

Crammond DJ, Kalaska JF. Prior information in motor and premotor cortex: activity during the delay period and effect on pre-movement activity. *J Neurophysiol* 84: 986–1005, 2000.

Dickey AS, Suminski A, Amit Y, Hatsopoulos NG. Single-unit stability using chronically implanted multielectrode arrays. *J Neurophysiol* 102: 1331–1339, 2009.

Dum RP, Strick PL. The origin of corticospinal projections from the premotor areas in the frontal lobe. *J Neurosci* 11: 667–689, 1991.

Dushanova JA, Donoghue JP. Neural activity in monkey primary motor cortex during action observation (Abstract). Program No. 57.6. *2006 Neuroscience Meeting Planner*.Atlanta, GA: Society for Neuroscience, 2006.

Dushanova J, Donoghue J. Neurons in primary motor cortex engaged during action observation. *Eur J Neurosci* 31: 386–398, 2010.

Evarts EV, Fromm C. Transcortical reflexes and servo control of movement. *Can J Physiol Pharmacol* 59: 757–775, 1981.

Evarts EV, Tanji J. Gating of motor cortex reflexes by prior instruction. *Brain Res* 71: 479–494, 1974.

Evarts EV, Tanji J. Reflex and intended responses in motor cortex pyramidal tract neurons of monkey. *J Neurophysiol* 39: 1069–1080, 1976.

Garcia-Rill E, Dubrovsky B. Responses of motor cortex cells to visual stimuli. *Brain Res* 82: 185–194, 1974.

Georgopoulos AP, Ashe J, Smyrnis N, Taira M. The motor cortex and the coding of force. *Science* 256: 1692–1695, 1992.

Georgopoulos AP, Kalaska JF, Caminiti R, Massey JT. On the relations between the direction of two-dimensional arm movements and cell discharge in primate motor cortex. *J Neurosci* 2: 1527–1537, 1982.

Georgopoulos AP, Taira M, Lukashin A. Cognitive neurophysiology of the motor cortex. *Science* 260: 47–52, 1993.

Hatsopoulos NG, Suminski AJ. Sensing with the motor cortex. *Neuron* 72: 477–487, 2011.

Hatsopoulos NG, Xu Q, Amit Y. Encoding of movement fragments in the motor cortex. *J Neurosci* 27: 5105–5114, 2007.

Hatsopoulos N, Joshi J, O'Leary JG. Decoding continuous and discrete motor behaviors using motor and premotor cortical ensembles. *J Neurophysiol* 92: 1165–1174, 2004.

He SQ, Dum RP, Strick PL. Topographic organization of corticospinal projections from the frontal lobe: Motor areas on the lateral surface of the hemisphere. *J Neurosci* 13: 952–980, 1993.

Hochberg LR, Serruya MD, Friehs GM, Mukand JA, Saleh M, Caplan AH, Branner A, Chen D, Penn RD, Donoghue JP. Neuronal ensemble control of prosthetic devices by a human with tetraplegia. *Nature* 442: 164–171, 2006.

Humphrey DR, Schmidt EM, Thompson WD. Predicting measures of motor performance from multiple cortical spike trains. *Science* 170: 758–762, 1970.

Kalaska JF, Crammond DJ. Cerebral cortical mechanisms of reaching movements. *Science* 255: 1517–1523, 1992. Retrieved from Google Scholar.

Kalaska JF, Scott SH, Cisek P, Sergio LE. Cortical control of reaching movements. *Curr Opin Neurobiol* 7: 849–859, 1997.

Lamarre Y, Busby L, Spidalieri G. Fast ballistic arm movements triggered by visual, auditory, and somesthetic stimuli in the monkey. I. Activity of precentral cortical neurons. *J Neurophysiol* 50: 1343–1358, 1983.

Merchant H, Battaglia-Mayer A, Georgopoulos AP. Effects of optic flow in motor cortex and area 7a. *J Neurophysiol* 86: 1937–1954, 2001.

Moritz CT, Perlmutter SI, Fetz EE. Direct control of paralysed muscles by cortical neurons. *Nature* 456: 639–642, 2008.

Morrow MM, Miller LE. Prediction of muscle activity by populations of sequentially recorded primary motor cortex neurons. *J Neurophysiol* 89: 2279–2288, 2003.

Mukamel R, Ekstrom AD, Kaplan J, Iacoboni M, Fried I. Single-neuron responses in humans during execution and observation of actions. *Curr Biol* 20: 750–756, 2010.

Mulliken GH, Musallam S, Andersen RA. Decoding trajectories from posterior parietal cortex ensembles. *J Neurosci* 28: 12913–12926, 2008.

Paz R, Vaadia E. Learning-induced improvement in encoding and decoding of specific movement directions by neurons in the primary motor cortex. *PLoS Biol* 2: e45, 2004.

Rathelot JA, Strick PL. Subdivisions of primary motor cortex based on cortico-motoneuronal cells. *Proc Natl Acad Sci USA* 106: 918–923, 2009.

Salinas E, Romo R. Conversion of sensory signals into motor commands in primary motor cortex. *J Neurosci* 18: 499–511, 1998.

Sanes JN, Donoghue JP. Plasticity and primary motor cortex. *Annu Rev Neurosci* 23: 393–415, 2000.

Schwartz AB, Cui XT, Weber DJ, Moran DW. Brain-controlled interfaces: movement restoration with neural prosthetics. *Neuron* 52: 205–220, 2006.

Schwartz AB, Moran DW, Reina GA. Differential representation of perception and action in the frontal cortex. *Science* 303: 380–383, 2004.

Scott SH. Apparatus for measuring and perturbing shoulder and elbow joint positions and torques during reaching. *J Neurosci Methods* 89: 119–127, 1999.

Scott SH. The role of primary motor cortex in goal-directed movements: insights from neurophysiological studies on non-human primates. *Curr Opin Neurobiol* 13: 671–677, 2003.

Seal J, Commenges D, Salamon R, Bioulac B. A statistical method for the estimation of neuronal response latency and its functional interpretation. *Brain Res* 278: 382–386, 1983.

Shen L, Alexander GE. Neural correlates of a spatial sensory-to-motor transformation in primary motor cortex. *J Neurophysiol* 77: 1171–1194, 1997.

Snyder LH, Batista AP, Andersen RA. Coding of intention in the posterior parietal cortex. *Nature* 386: 167–170, 1997.

Suner S, Fellows MR, Vargas-Irwin C, Nakata GK, Donoghue JP. Reliability of signals from a chronically implanted, silicon-based electrode array in non-human primate primary motor cortex. *IEEE Trans Neural Syst Rehabil Eng* 13: 524–541, 2005.

Tanji J, Evarts EV. Anticipatory activity of motor cortex neurons in relation to direction of an intended movement. *J Neurophysiol* 39: 1062–1068, 1976.

Thoroughman KA, Shadmehr R. Electromyographic correlates of learning an internal model of reaching movements. *J Neurosci* 19: 8573–8588, 1999.

Tkach D, Reimer J, Hatsopoulos NG. Congruent activity during action and action observation in motor cortex. *J Neurosci* 27: 13241–13250, 2007.

Tkach D, Reimer J, Hatsopoulos NG. Observation-based learning for brain-machine interfaces. *Curr Opin Neurobiol* 18: 589–594, 2008.

Vargas-Irwin CE, Shakhnarovich G, Yadollahpour P, Mislow JM, Black MJ, Donoghue JP. Decoding complete reach and grasp actions from local primary motor cortex populations. *J Neurosci* 30: 9659–9669, 2010.

Vargas-Irwin C, Donoghue JP. Automated spike sorting using density grid contour clustering and subtractive waveform decomposition. *J Neurosci Methods* 164: 1–18, 2007.

Wannier TMJ, Maier MA, Hepp-Reymond MC. Responses of motor cortex neurons to visual stimulation in the alert monkey. *Neurosci Lett* 98: 63–68, 1989.

West WR, Ogden TR. Continuous-time estimation of a change-point in a Poisson process. *J Stat Comput Simul* 56: 293–302, 1997.

Wolpert DM, Ghahramani Z. Computational principles of movement neuroscience. *Nat Neurosci* 3: 1212–1217, 2000.

Wolpert DM, Ghahramani Z, Jordan MI. An internal model for sensorimotor integration. *Science* 269: 1880–1882, 1995.

Yu B, Afshar A, Santhanam G, Ryu SI, Shenoy K, Sahani M. Extracting dynamical structure embedded in neural activity. *Adv Neural Inf Process Syst* 18: 1545–1552, 2006.